Quantum Mechanical Rippling of a MoS_{2} Monolayer Controlled by Interlayer Bilayer Coupling

Yi Zheng, Jianyi Chen, M.-F. Ng, Hai Xu, Yan Peng Liu, Ang Li, Sean J. O'Shea, T. Dumitrică, and Kian Ping Loh

Phys. Rev. Lett. **114**, 065501 — Published 10 February 2015

DOI: 10.1103/PhysRevLett.114.065501

Quantum mechanical rippling of MoS_2 monolayer controlled by interlayer bilayer coupling

Yi Zheng,[1,2,*] Jianyi Chen,[1,*] M. -F. Ng,[3] Yan Peng Liu,[1] Ang Li,[4] Sean J. O'Shea,[5] T. Dumitrică,[6] and Kian Ping Loh[1,2,†]

[1]*Department of Chemistry, National University of Singapore, 3 Science Drive 3, Singapore 117543*

[2]*Graphene Research Center, 6 Science Drive 2, National University of Singapore, Singapore 117546*

[3]*Institute of High Performance Computing, Agency for Science, Technology and Research, 1 Fusionopolis Way, #16-16 Helios, Singapore 138632*

[4]*Bruker Singapore, 11 Biopolis Way #10-10 Helios, Singapore 138667*

[5]*Institute of Materials Research and Engineering, Agency for Science, Technology and Research, 3 Research Link, Singapore 117602*

[6]*Department of Mechanical Engineering, University of Minnesota, Minneapolis, Minnesota 55455,USA*

(Dated: January 29, 2015)

Abstract

Nanoscale corrugations are of great importance in determining the physical properties of two-dimensional crystals. However, the mechanical behavior of atomically thin films under strain is not fully understood. In this letter, we show layer-dependent mechanical response of molybdenum disulfide (MoS_2) subject to atomistic-precision strain induced by 2H-bilayer island epitaxy. Dimensional crossover in the mechanical properties is evidenced by the formation of star-shaped nanoripple arrays in the first monolayer, while rippling instability is completely suppressed in the bilayer. Microscopic-level quantum mechanical simulations reveals that the nanoscale rippling is realised by the twisting of neighboring Mo-S bonds without modifying the chemical bond length, and thus invalidates the classical continuum mechanics. The formation of nanoripple arrays significantly changes the electronic and nanotribological properties of monolayer MoS_2. Our results suggest that quantum mechanical behavior is not unique for sp^2 bonding but general for atomic membranes under strain.

* These authors contributed equally to this work.

† chmlohkp@nus.edu.sg

The physical properties of two-dimensional (2D) crystals are closely related to the atomic layer numbers, as interlayer coupling drives the dimensional crossover from 2D to bulk physics when the thickness increases discretely. Interlayer coupling leads to the striking transitions in quantum phenomena, from the massless Dirac fermions in monolayer (ML) graphene[1,2] to the massive chiral fermions in bilayer graphene[3]. In MoS_2, interlayer coupling is responsible for the crossover from a direct bandgap semiconductor in the ML to an indirect bandgap material in the bulk[4]. However, the influence of interlayer coupling on the mechanical behaviours of atomically thin 2D crystals remains less understood. Particularly, ML graphene and MoS_2 show extremely small bending rigidity (κ)[5–7] and exceptionally high Young's modulus (E)[8,9]. Such coexistence of extreme out-of-plane flexibility and in-plane stiffness is quite unusual, considering that classical elasticity theory correlates E and κ by the relation $\kappa = \frac{Eh_e^3}{12(1-\nu^2)}$, in which h_e and ν are elastic thickness and the Poisson ratio, respectively[10]. In the 2D limit, this continuum plate model has been challenged by theory[11] and experiment[12]. The observed subnanometer-scale rippling of graphene[12] originates in the decoupling of the bending and tensional deformations and hence invalidates the above relation. Bao *et al.* reported that at variance sub-micrometer ripple texture formation in suspended few-layer graphene follows the classical elasticity theory[13]. To understand elasticity in the 2D limit, the layer-dependent mechanical response of 2D crystals to strain must be studied. More importantly, as the decoupling of the bending and tensional deformations in graphene is unique for sp^2 hybridization, it is interesting to investigate whether non-classical rippling phenomena are valid for other 2D-crystal MLs, such as in transitional metal dichalcogenides (TMDCs).

In this letter, we use centrosymmetric triangular-shaped MoS_2 epilayers as a model system to study layer-dependent mechanical properties of 2D crystals. The centrosymmetric bilayer (BL) island epitaxy on the first ML induces an atomistic-precision biaxial strain at the ML-BL boundaries by the interlayer edge-to-basal plane coupling. With the 2H stacking symmetry, we observe star-shaped strain patterns of one-dimensional nanoripple arrays (1D NRAs) in the ML, in contrast to the non-rippling BL island. We show that such nanoscale rippling phenomena violate the classical continuum mechanics, and its origin can be traced to the quantum-mechanical behaviour of 2D-crystal MLs. The formation of nanoripple arrays effectively modifies the physical properties of ML MoS_2, affording new strategies in electronic, strain and friction engineering in ML TMDCs.

The detailed chemical vapor growth of centrosymmetric MoS_2 epilayers is described in the Supplemental Material[14]. Here, centrosymmetric growth is used to denote the growth of a second atomic-layer island on top of the first ML, both sharing the same nucleation center. Strain pattern formation in MoS_2 epilayers with two distinct stacking symmetry of 2H and 3R[15] has been characterized by multiple atomic force microscopy techniques, Raman and photoluminescence (PL).

In Figure 1a, friction force microscopy (FFM) highlights the characteristic 3-fold strain patterns of 1D NRAs in the MoS_2 ML induced by 2H BL island growth. Dimensional crossover in the mechanical properties from the first ML to BL can be clearly seen, as rippling instability is completely suppressed in the BL. The formation of 1D NRAs is closely correlated to the sudden increase in κ from ML to BL MoS_2 island. For few-layer graphene, density functional-based tight-binding (DFTB) model predicts an $N(N^2-1)$ scaling of κ with the number of layers N. For $N = 1$, the bending resistance is completely determined by the quantum mechanical π-orbital misalignment, decoupled from in-plane σ-bond stretching[11]. For non-sp^2 MoS_2 ML, consisting of three sub-monolayers in the sandwiched structure of S-Mo-S connected by covalent bonds[14], such a microscopic model does not apply. However, MoS_2 ML is also known to have an extremely low κ of a few eV[8,9,16], and thus MoS_2 ML is expected to be slightly stretched on the rough SiO_2 surface. The formation of a centrosymmetric BL increases κ by at least an order of magnitude, even within the framework of the classical theory. The abrupt change in κ at the interface between the ML and BL created a restoring force on the stretched lattices, exerted by the more rigid bilayer[14]. Consequently, a 3-fold biaxial strain was created in the first ML, which was stretched along the angle-bisector directions and compressed along the ML-BL boundaries. Poisson instability induced by the compressive strain leads to out-of-plane rippling[10], which propagates along the tensile strain direction to form 1D NRAs[17]. Due to the inner symmetry of 2H stacking, 1D NRA formation are three folded along each angle-bisector direction to form a star-shaped strain pattern (Figure 1a).

The strength of such biaxial strain can be estimated by first principle density functional theory (DFT) calculations[14]. In Figure 1b, we simulated centrosymmetric 2H-MoS_2 bilayer growth on a fully relaxed ML consisting of 227 atoms. We found that the interlayer coupling induces $\sim 1.1\%$ compressive strain in the vicinity of ML-BL boundaries, and $\sim 0.5\%$ tensile strain along the angle-bisector directions. Microscopically, the compressive strain originates

from the competition between interlayer Coulomb attraction between S and Mo atoms and Pauli repulsion between S atoms at the ML-BL boundaries. In 2H-MoS_2, the interlayer nearest-neighbor S-S repulsion force is perpendicular to the boundaries. Along the edge direction, interlayer coupling is dominated by S-Mo Coulomb interaction[14]. The bottom ML responses to the shearing Coulomb attraction by twisting the Mo-S bond, creating the compressive strain (see the quantum mechanical simulation below)[18].

Intriguingly, 1D NRAs are absent in 3R-MoS_2 crystals. Our DFT simulation reveals that centrosymmetric 3R bilayer growth induces $\sim 0.4\%$ tensile strain along the ML-BL boundaries (Figure 1c). The transition from compressive strain in 2H-MoS_2 to tensile strain in 3R-MoS_2 explains the absence of 1D NRAs in the latter, since compressive strain is essential for rippling phenomena[17]. The tensile strain originates in the edge structure of the 3R-BL, in which the interlayer nearest-neighbor S atoms are arranged in a zigzag pattern[14]. Furthermore, in 3R-MoS_2, Mo atoms are in the hollow sites of the first ML. Such an arrangement also enhances the tensile strain by S-Mo attraction. The dominance of the Pauli repulsion force along the 3R-MoS_2 interlayer edges is manifested by the interlayer nearest-neighbor S-S distance, which is ~ 0.1 Å longer than 2H-MoS_2[14]. Detailed in-plane and interplane lattice changes for 2H and 3R-BL growth can be found in Supplemental Material[14].

The physical existence of 1D NRAs was also confirmed by amplitude-modulation non-contact AFM (NCAFM) and force-modulation AFM (FMAFM). The former utilises attractive forces and does not exert compressive force on nanoripples[14], and the latter was applied to study the morphology changes of nanoripples as a function of peak tapping force. Using a peak force of 50 pN, the tip-surface interaction was minimized and the intrinsic surface morphology of 1D NRAs was imaged (Figure 2a and 2b). By increasing the setting to 500 pN, nanoripples become noticeably blurred due to ripple deformation under increased tip compression (Figure 2c). Further increasing the peak tapping force gradually made the 1D NRAs indiscernible, as shown in Figure 2d (1 nN) and Figure 2e (4 nN). Uniquely, FMAFM also allowed us to record the local elastic deformation at the peak-force setpoint during the topographic acquisition. Using the stiffer BL as a reference, the MoS_2 ML deformed an extra 0.25 nm on average at a force load of 4 nN, while the buckled nanoripple arrays deformed 0.35 nm[14].

We determined the physical dimensions of 1D NRAs by FFM, NCAFM, and FMAFM with good consistency[19]. Typical cross-section profiles of 1D NRAs are shown in Figure 3a

(the solid red and black lines), with an average nanoripple amplitude of $A \sim 1$ nm, in contrast to featureless non-rippled MoS_2 ML (the dashed black line). The nanoripple amplitude is relatively constant over the entire strained area and is independent of the dimension of the 2H-BL. However, the presence of a rigid substrate induces a perturbation to the periodicity of the 1D NRAs, as revealed by fast Fourier transformed (FFT) topographic images. The FFT of Figure 2b shows two main sets of periodicity, multiples of 23 nm and 26 nm[14]. Each peak is significantly broadened and has satellite peaks. Nevertheless, the basic periodicity of 1D NRAs obtained from different 2H crystals using FFM, NCAFM and FMAFM converges in the range of $21-26$ nm, which cannot be explained by MoS_2-substrate coupling, considering the amorphous nature of SiO_2. More importantly, 1D NRAs are absent in pure ML and 3R-MoS_2, which constitute 76% of all the grown crystals[14]. We have also observed quadruple MoS_2 crystals stacked in 3R-3R-2H sequences from bottom to top. The emergence of 1D NRAs in the third ML due to 2H-coupling with the fourth ML provide the convincing evidences in the atomic origin of the interlayer edge-to-basal plane coupling[14].

We compared the 1D NRAs on MoS_2 with the experimental reports on periodic ripples in graphene. In Ref. 13, Bao *et al.* studied the formation of 1D periodical ripples in suspended graphene membranes induced by thermal treatment. Their report claims that ripple formation in atomically thin films follows the classical elasticity theory, which correlates A, wavelength (λ), and the thickness of atomic membrane (t) as,

$$\lambda = \frac{(2\pi Lt)^{\frac{1}{2}}}{[3(1-\nu^2)\gamma]^{\frac{1}{4}}}; A = (\nu Lt)^{\frac{1}{2}}[\frac{16\gamma}{3\pi^2(1-\nu^2)}]^{\frac{1}{4}}, \quad (1)$$

where L is the length of suspended channel, and γ is the tensile strain induced by thermal treatment. By eliminating the sample-dependent γ, the classical theory requires A, λ and t to satisfy a constant condition:

$$\frac{A\lambda}{Lt} = \sqrt{\frac{8\nu}{3(1-\nu^2)}}. \quad (2)$$

These equations describe the micrometer-sized ripple in Ref. 13, in which λ ranges from 0.37 to 5 μm. However, the applicability of classical elasticity theory to 2D MLs has been challenged by periodic subnanometer-wavelength rippling in suspended graphene ML grown on Cu(111)[12]. At this length scale, which is close to the lattice constant of graphene, $\frac{A\lambda}{Lt}$ is smaller than $\sqrt{\frac{8\nu}{3(1-\nu^2)}}$ by more than an order of magnitude. We found that the classical elastic theory is also violated by the physical dimensions of the 1D NRAs in 2H-MoS_2

multilayers. Taking $A = 1$ nm, $\lambda = 23$ nm, $L = 1$ μm, $t = 0.46$ nm and $\nu = 0.26$[20], the relation in Equation 2 fails by at least a factor of ten. Alternatively, we can use Equation 2 to calculate an equivalent plate thickness to match the experimental observations. The deduced equivalent t is 0.17 Å, which is certainly unrealistic[14].

We confirmed the quantum mechanical origin of rippling in ML MoS_2 with microscopic-level simulations using DFTB[16]. A simulation domain containing 144 atoms was placed under periodic boundary conditions along the $x - y$ in-plane directions. Compressive strain was applied by a protocol that gradually varied the periodicity along the x direction followed by conjugate gradient relaxation simulations[14]. In contrast to the classical modeling, we found that the microscopic approach can reproduce the nanometer-scale rippling observed in our AFM studies. Indeed, Figure 3b shows a periodic rippling exhibited by the MoS_2 ML with a wavelength of 12.7 nm and amplitude of 0.95 nm, in excellent agreement with the experimental measurements presented in Figure 3a. The analysis of the bond lengths shown in the inset offers an intuitive explanation for the violation of the plate behavior. The classical bending of plate involves asymmetrical stretching and compression on material located on the opposite sides of the neutral line. In contrast, the Mo-S bonds located in the concave and convex regions of the ripple are practically identical in length. This is because the S atoms are free to move along the out-of-plane direction to relax the strain in the Mo-S bonds. Thus, although in the S-Mo-S trilayer, MoS_2 can still easily curve because of its microscopic structure, which allows the twisting of neighboring Mo-S bonds without modifying the chemical bond length.

Using Raman and PL, we qualitatively determined the strain type and strain intensity of the 1D NRAs. For Raman (Figure 4a and 4b), we selected twinned crystals with the concentric bilayer growth located on the right twin[14]. In Raman mapping, significant phonon hardening was observed, as manifested by blue shifts in both in-plane (E^1_{2g}) and out-of-plane (A_{1g}) vibration modes (Figure 4a). Based on the Raman shift of $\sim$2 cm^{-1} for A_{1g} (Figure 4b), we estimate the corresponding average compressive strain is about 1%[21,22]. This compares favorably to the strains estimated from the DFT calculations in Figure 1b. The compressive nature of the strain formed in 1D NRAs is also confirmed by the narrowing of the full width at half maximum (FWHM) of both E^1_{2g} and A_{1g} peaks (Figure 4b). The estimated strain intensity agrees well with the PL experiment, which indicates an equivalent strain of $\sim$0.7% based on a 41 meV change in PL peak positions[23] (Figure 4c and 4d). Therefore, both

Raman and PL results support the microscopic origin of the biaxial strain from interlayer coupling, as revealed by the DFT simulation.

Our studies show that an atomistic rippling instability induced by strong interlayer edge-to-basal plane coupling causes quantum mechanical rippling phenomena in MoS_2 ML, but does not influence the BL. Such atomistic rippling instability is unique in its dependence on geometrical bilayer stacking and the pronounced 3-fold symmetry, which are fundamentally different from the previously reported nanorippling instability in 2D material, such as strain accumulation at the grain boundaries[14,24]. The results provide direct evidence on layer-dependent mechanical properties of 2D crystals, and suggest quantum mechanical rippling that violates classical mechanics may be generic to 2D MLs. Despite the atomistic origin, 1D NRAs show robust resistance to perturbation by a rough SiO_2 substrate and can extend for tens of micrometers along the tensile strain direction. This opens the possibility for micro/nano device fabrications, in which 1D NRAs are utilised as active channels. Centrosymmetric bilayer epitaxy may also provide an efficient way to form 2D van der Waals heterostructures[25] and 1D topological defects, such as soliton-like strain boundaries[26,27].

ACKNOWLEDGEMENTS

We thank Antonio Castro-Neto, Jens Martin and Hai Xu for insightful discussions. We acknowledge funding support from National Research Foundation CRP award "Plasmon Electronics, New Generation of Devices to Bypass Fundamental Limitations". The DFT simulations were supported by the A*STAR Computational Resource Centre (ACRC) in Singapore through the use of its high performance computing facilities. T.D. acknowledges funding support from NSF 1006706.

---

[1] K. S. Novoselov, A. K. Geim, S. V. Morozov, D. Jiang, M. I. Katsnelson, I. V. Grigorieva, S. V. Dubonos, and A. A. Firsov, "Two-dimensional gas of massless Dirac fermions in graphene," Nature **438**, 197–200 (2005).

[2] Y. Zhang, Y. W. Tan, H. L. Stormer, and P. Kim, "Experimental observation of the quantum Hall effect and Berry's phase in graphene," Nature **438**, 201–204 (2005).

[3] K. S. Novoselov, E. Mccann, S. V. Morozov, V. I. Fal'ko, M. I. Katsnelson, U. Zeitler, D. Jiang, F. Schedin, and A. K. Geim, "Unconventional quantun Hall effect and Berry's phase of 2π in bilayer graphene," Nature Phys. **2**, 177–180 (2006).

[4] K. F. Mak, C. Lee, J. Hone, J. Shan, and T. F. Heinz, "Atomically thin MoS_2: A new direct-gap semiconductor," Phys. Rev. Lett. **105**, 136805 (2010).

[5] C. Lee, X. Wei, J. W. Kysar, and J. Hone, "Measurement of the elastic properties and intrinsic strength of monolayer graphene," Science **321**, 385–388 (2008).

[6] P. Johari and V. B. Shenoy, "Tuning the electronic properties of semiconducting transition metal dichalcogenides by applying mechanical strains," ACS Nano **6**, 5449–5456 (2012).

[7] A. Castellanos-Gomez, M. Poot, G. A. Steele, H. S. J. van der Zant, N. Agrait, and G. Rubio-Bollinger, "Elastic properties of freely suspended MoS_2 nanosheets," Adv. Mater. **24**, 772–775 (2012).

[8] Y. Wei, B. Wang, J. Wu, R. Yang, and M. L. Dunn, "Bending rigidity and Gaussian bending stiffness of single-layered graphene," Nano Lett. **13**, 26–30 (2013).

[9] N. Lindahl, D. Midtvedt, J. Svensson, O. L. Nerushev, N. Lindvall, A. Isacsson, and E. E. B. Campbell, "Determination of the bending rigidity of graphene via electrostatic actuation of buckled membranes," Nano Lett. **12**, 3526–3531 (2012).

[10] L. D. Landau and E. M. Lifshitz, *Theory of Elasticity* (Pergamon Press, 1970).

[11] D. B. Zhang, E. Akatyeva, and T. Dumitrică, "Bending ultrathin graphene at the margins of continuum mechanics," Phys. Rev. Lett. **106**, 255503 (2011).

[12] L. Tapaszto, T. Dumitrica, S. J. Kim, P. Nemes-Incze, C. Hwang, and L. P. Biro, "Breakdown of continuum mechanics for nanometer-wavelength rippling of graphene," Nature Phys. **8**, 739–742 (2012).

[13] W. Bao, F. Miao, Z. Chen, H. Zhang, W. Jang, C. Dames, and C. N. Lau, "Controlled ripple texturing of suspended graphene and ultrathin graphite membranes," Nature Nano. **4**, 562–566 (2009).

[14] See Supplemental Material at http://link.aps.org/supplemental/, which includes Ref. [28-38], for CVD growth and DFT calculations.

[15] H. Bergmann, B. Czeska, I. Haas, B. Mohsin, and K. H. Wandner, *Gmelin Handbook of Inorganic and Organometallic Chemistry* (Springer-Verlag: Berlin, 1992).

[16] D. B. Zhang, T. Dumitrică, and G. Seifert, "Helical nanotube structures of mos_2 with intrinsic twisting: An objective molecular dynamics study," Phys. Rev. Lett. **104**, 065502 (2011).

[17] E. Cerda and L. Mahadevan, "Geometry and physics of wrinkling," Phys. Rev. Lett. **90**, 074302 (2003).

[18] It is noteworthy that the biaxial strain is underestimated in the DFT simulation because the effects of substrate roughness are excluded from the calculation. Furthermore, the MoS_2 epilayer had a much larger thermal expansion coefficient than the SiO_2 substrate [J. Appl. Cryst. 9, 403 (1976)]. During crystal growth, there was significant tensile strain build-up, which was pinned by MoS_2-substrate interactions.

[19] 1D NRAs are not visible in the contact AFM (CAFM) topographic images, indicating that there is substantial elastic deformation of nanoripples in contact mode. In contrast, FFM was enhanced by the localised compression and deformation of 1D NRAs when the tip moving across the rippled textures. The dominant friction interaction between the 2D-cyrstal ML and the CAFM tip has been reported previously, showing that kinetic friction is increased by a factor of two to three due to the out-of-plane deformation of atomically thin films [Science 328, 76 (2010)]. Here, by forming 1D NRAs, kinetic friction was further increased by about two times, mainly due to the large elastic deformation of the nanoripples.

[20] J. L. Feldman, "Elastic constants of 2H-MoS_2 and 2H-$NbSe_2$ extracted from measured dispersion curves and linear compressibilities," J. Phys. Chem. Solids **37**, 1141–1144 (1976).

[21] K. He, C. Poole, K. F. Mak, and J. Shan, "Experimental demonstration of continuous electronic structure tuning via strain in atomically thin MoS_2," Nano Lett. **13**, 2931–2936 (2013).

[22] Y. Y. Hui, X. Liu, W. Jie, N. Y. Chan, J. Hao, Y. Hsu, L. Li, W. Gao, and S. P. Lau, "Exceptional tunability of band energy in a compressively strained trilayer MoS_2 sheet," ACS Nano **7**, 7126–7131 (2013).

[23] H. J. Conley, B. Wang, J. I. Ziegler, R. F. Haglund, Jr., S. T. Pantelides, and K. I. Bolotin, "Bandgap engineering of strained monolayer and bilayer MoS_2," Nano Lett. **13**, 3626–3630 (2013).

[24] P. Yeh, W. Jin, and N. Zaki et al., "Probing substrate-dependent long-range surface structure of single-layer and multilayer MoS_2 by low-energy electron microscopy and microprobe diffraction," Phys. Rev. B **89**, 186101 (2014).

[25] A. K. Geim and I. V. Grigorieva, "Van der Waals heterostructures," Nature **499**, 419–425 (2013).

[26] C. R. Woods, L. Britnell, A. Eckmann, R. S. Ma, J. C. Lu, H. M. Guo, X. Lin, G. L. Yu, Y. Cao, R. V. Gorbachev A. V. Kretinin, J. Park, L. A. Ponomarenko, M. I. Katsnelson, Yu. N. Gornostyrev, K. Watanabe, T. Taniguchi, C. Casiraghi, H. J. Gao, A. K. Geim, and K. S. Novoselov, "Commensurate-incommensurate transition in graphene on hexagonal boron nitride," Nature Phys. **10**, 451–456 (2014).

[27] J. S. Alden, A. W. Tsen, P. Y. Huang, R. Hovden, L. Brown, J. Park, D. A. Muller, and P. L. McEuen, "Strain solitons and topological defects in bilayer graphene," Proc. Natl. Acad. Sci. U.S.A. **110**, 11256–11260 (2013).

[28] I. Horcas, R. Fernández, and J. M. Gómez-Rodriguez and J. Colchero and J. Gómez-Herrero and A. M. Baro, "WsXM: A software for scanning probe microscopy and a tool for nanotechnology," Rev. Sci. Instrum. **78**, 013705 (2007).

[29] B. B. Pittenger, N. Erina, and C. Su, *Quantitative mechanical property mapping at the nanoscale with PeakForce QNM* (Bruker, 2012).

[30] J. P. Perdew, K. Burke, and M. Ernzerhof, "Generalized gradient approximation made simple," Phys. Rev. Lett. **77**, 3865 (1996).

[31] S. Grimme, "Semiempirical gga-type density functional constructed with a long-range dispersion correction," J. Comp. Chem. **27**, 1787–1799 (2006).

[32] G. Kresse and J. Furthmüller, "Efficiency of ab-initio total energy calculations for metals and semiconductors using a plane-wave basis set," Comput. Mater. Sci. **6**, 15–50 (1996).

[33] G. Kresse and J. Furthmüller, "Efficiency of ab-initio total energy calculations for metals and semiconductors using a plane-wave basis set," Phys. Rev. B **54**, 11169 (1996).

[34] P. E. Blöchl, "Projector augmented-wave method," Phys. Rev. B **50**, 17953 (1994).

[35] A. Socoliuc, E. Gnecco, S. Maier, O. Pfeiffer, A. Baratoff, R. Bennewitz, and E. Meyer, "Atomic-scale control of friction by actuation of nanometer-sized contacts," Science **313**, 207–210 (2006).

[36] M. Dienwiebel, G. S. Verhoeven, N. Pradeep, J. W. M. Frenken, J. A. Heimberg, and H. W. Zandbergen, "Superlubricity of graphite," Phys. Rev. Lett. **92**, 126101 (2004).

[37] X. S. Li, W. Cai, J. An, S. Kim, J. Nah, D. Yang, R. Piner, A. Velamakanni, I. Jung, E. Tutuc, S. K. Banerjee, L. Colombo, and R. S. Ruoff, "Large-area synthesis of high-quality

and uniform graphene films on copper foils," Science **324**, 1312–1314 (2009).

[38] G. X. Ni, Y. Zheng, S. Bae, H. R. Kim, A. Pachoud, Y. S. Kim, C. L. Tan, D. Im, J. H. Ahn, B. H. Hong, and B. Özyilmaz, "Quasi-periodic nanoripples in graphene grown by chemical vapor deposition and its impact on charge transport," ACS Nano **6**, 1158–1164 (2012).

FIGURES

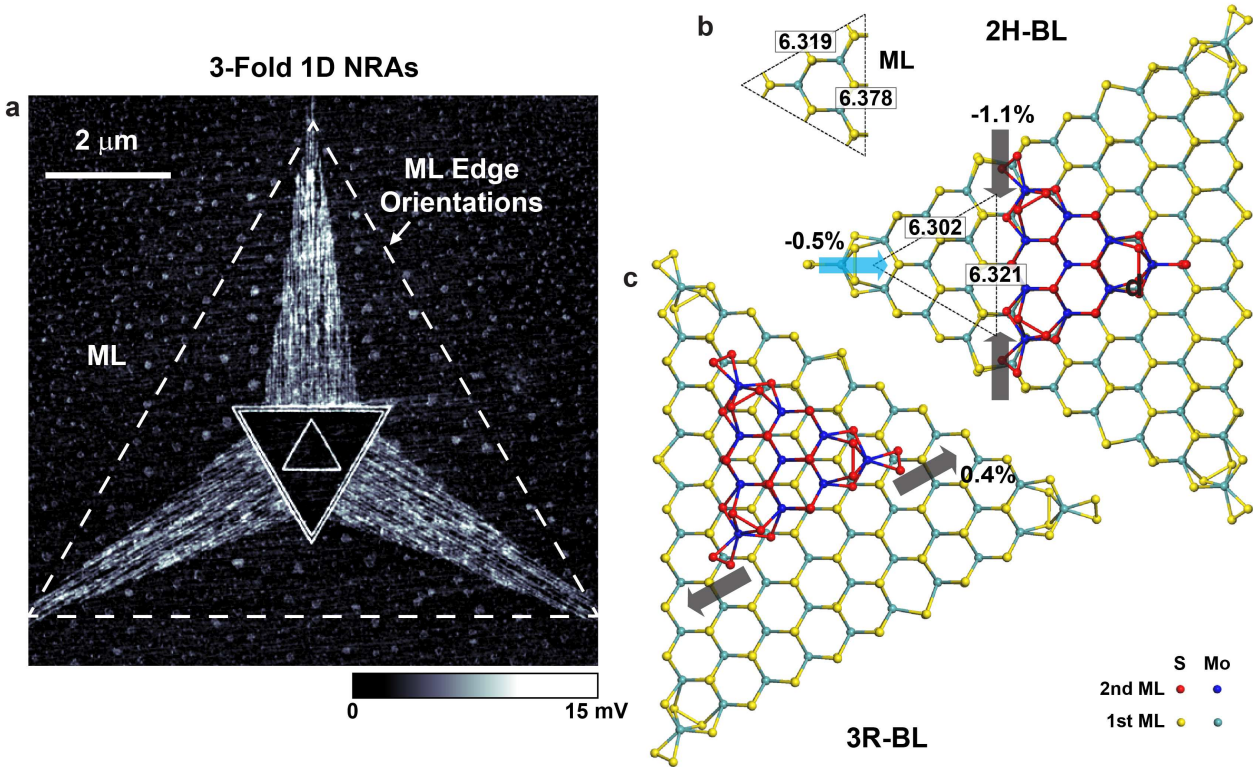

FIG. 1. Atomistic origin of 1D NRAs in MoS_2 ML induced by centrosymmetric 2H-BL growth. (a) Characteristic FFM image of 1D NRAs in MoS_2 ML. Normal force setpoint: 1 nN. (b) and (c) DFT simulation of 2H-BL and 3R-BL growth on a fully relaxed ML, respectively. 2H-BL induces compressive strain at the ML-BL boundaries, in contrast to tensile strain by 3R-BL. Lattice changes are in Å.

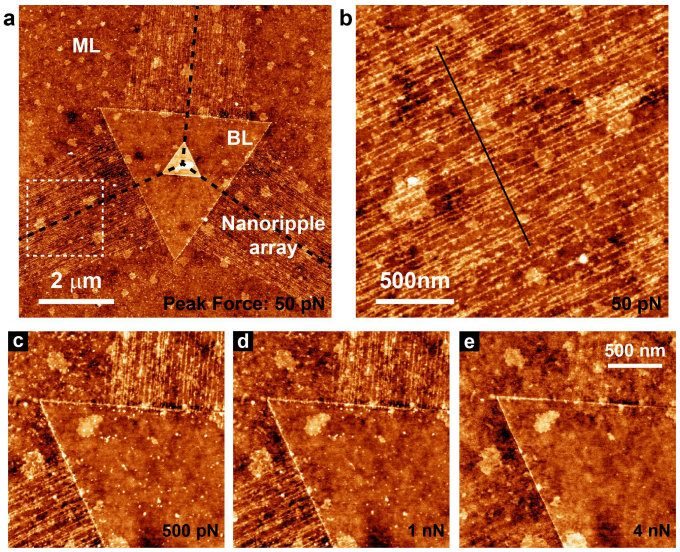

FIG. 2. Peak force-dependent FMAFM of 1D NRAs. (a) Star-shaped 1D NRAs formed along the three angle-bisector directions (indicated by the black dashed lines) of the ML due to the 2H-BL growth. (b) Zoom-in over the dashed square in Fig. 2(a). The black line are the position for the cross-section in Fig. 3a. (c)-(e) Nanoripple morphology at 500 pN, 1 nN and 4 nN peak-force, respectively. Color scale: $0-2.4$ nm for (a) and (b), and $0-2$ nm for (c)-(e) from black to white.

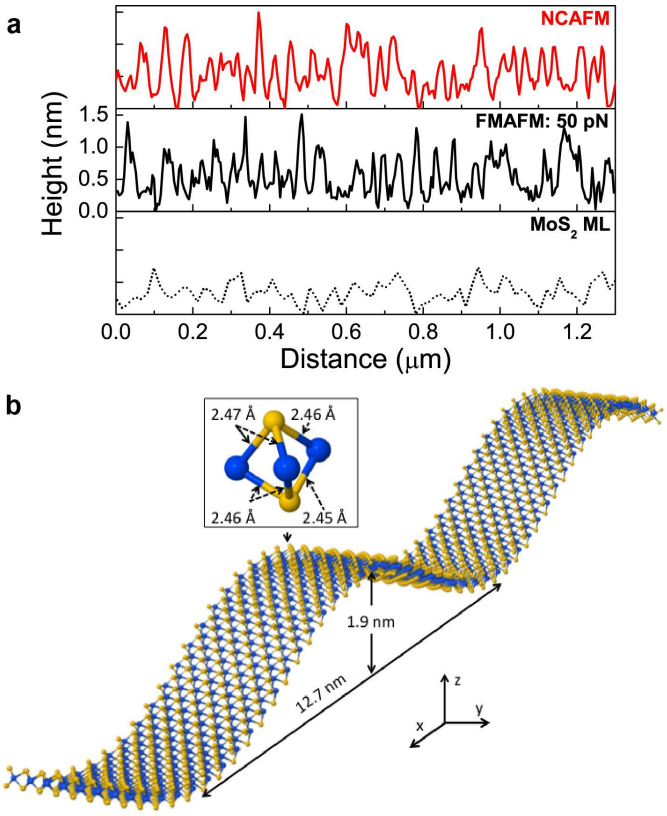

FIG. 3. Quantum mechanical simulation of 1D NRAs formation in MoS_2 ML. (a) Corrugations of 1D NRAs compared with non-rippled MoS_2 ML. (b) Atomistic simulation of a 1D NRA showing amplitude and wavelength matching the experiments. Inset shows the Mo-S bond lengths at the maximum amplitude location. The top (bottom) S atoms are located in the convex (concave) region of the ripple.

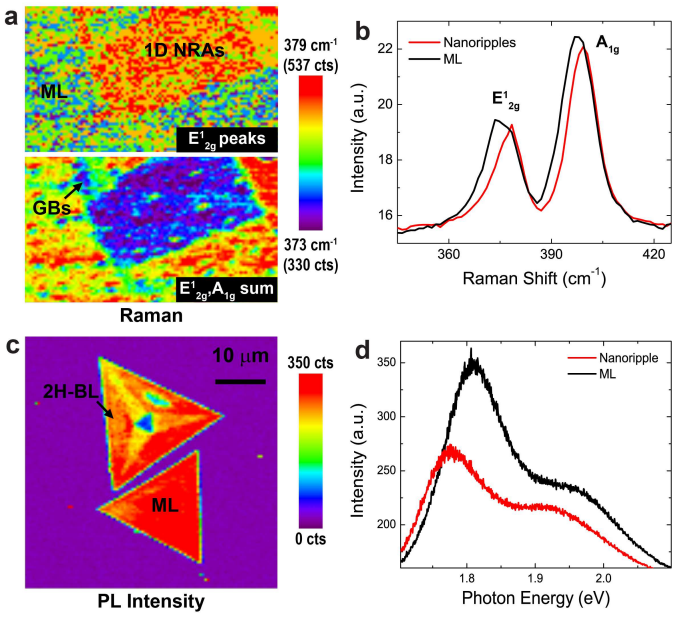

FIG. 4. (a) and (b) Raman characterizations of 1D NRAs formed in twinned crystals. The average stain intensity is estimated as ∼1%. (c) and (d) PL measurements of 1D NRAs. The measured shift in photon energy peaks agrees with the Raman results.